THE JOURNAL OF PHYSICAL CHEMISTRY B



Article

# Structural Analysis of [ChCl][ZnCl] Ionic Liquid by X-ray Absorption Fine Structure Spectroscopy

Yang Zou, Hongjie Xu, Guozhong Wu, Zheng Jiang, Shimou Chen, Yuying Huang, Wei Huang, and Xiangjun Wei

*J. Phys. Chem. B*, **2009**, 113 (7), 2066-2070• Publication Date (Web): 27 January 2009

# Structural Analysis of $[ChCl]_m[ZnCl_2]_n$ Ionic Liquid by X-ray Absorption Fine Structure Spectroscopy

**Yang Zou, Hongjie Xu,* Guozhong Wu,* Zheng Jiang, Shimou Chen, Yuying Huang, Wei Huang, and Xiangjun Wei**

*Shanghai Institute of Applied Physics, Chinese Academy of Sciences, Shanghai, China*

*Received: November 6, 2008; Revised Manuscript Received: December 12, 2008*

The components and structures of ionic liquid $ChCl-ZnCl_2$ in different $ChCl:ZnCl_2$ ratios were investigated using XAFS (X-ray absorption fine structure) technique. The average coordination number and distance of Zn species at different $x(ZnCl_2)$ (mole fraction of $ZnCl_2$ when synthesizing) were calculated. It is shown that $x(ZnCl_2)$ has a regular influence on the coordination number of Zn species, due to the change of anion forms and structures in the $ChCl-ZnCl_2$ ionic liquid. The possible forms and structures of Zn species in the ionic liquids were analyzed according to the coordination number. XAFS and DSC (differential scanning calorimetry) analysis imply that besides $ZnCl_3^-$ and $Zn_2Cl_5^-$ anions, the Cl−Zn−Cl ion pair is a main species in the ionic liquid at higher $x(ZnCl_2)$. This newly discovered Zn species has substantial influence on the properties of the ionic liquid. From the analysis of the coordination numbers and coordination distance, a new mechanism of interactions between $Ch^+$ cation and Cl−Zn−Cl ion pairs or $Cl^-$ is proposed.

## 1. Introduction

Room temperature ionic liquids (RTILs) possess many desirable chemical and physical properties, such as good solubility, large liquid temperature ranges, negligible vapor pressure, high ionic conductivities, and wide electrochemical window.[1−6] These characteristics of RTILs account for the increasing interest in application of RTILs.[7] As a substitute for volatile organic solvents, RTILs are considered to be a class of novel potential mediums in green chemistry.[8] RTILs can be designed with variable physicochemical properties by altering their cations and anions. Knowledge of the intrinsic component and structure of RTILs is important in understanding their properties and designing new RTILs.[9,10]

RTILs based on choline chloride and metals are easy to prepare and low in cost.[11] This class of ionic liquids may be used in electroplating and in batteries.[12,13] Components and properties of $ChCl-ZnCl_2$ RTILs at different $x(ZnCl_2)$ have previously been studied.[11,14] Abbott et al.[11] found that there are two main anions in this RTIL by FAB-MS (negative ion fast atom bombardment mass spectra), namely $ZnCl_3^-$ and $Zn_2Cl_5^-$. The group also measured the potential, melting point, viscosity, and mole fraction of chlorozinc anions in the ionic liquids prepared at different $x(ZnCl_2)$. Wu et al.[14] investigated the melting point and crystal morphology of this kind of RTILs and found that the melting point and crystal morphology were determined by $x(ZnCl_2)$. Hsiu et al. studied the component of ionic liquid $ZnCl_2$−1-ethyl-3-methylimidazolium chloride by FAB-MS and also found that there were many kinds of Zn anions in the ionic liquid, but the two main species were $ZnCl_3^-$ and $Zn_2Cl_5^-$.[15] Abbott et al.[16,17] also investigated the solubility of many metal oxides in $ChCl-ZnCl_2$ ionic liquids. Although many studies have been performed on $ChCl-ZnCl_2$ ionic liquids, XAFS is rarely used in studying ion structure of RTILs, and there are very few reports in which XAFS is employed to study this kind of novel material.[18−20] Jensen et al.[18] investigated the coordination environment of Sr atom in the extraction by RTIL. Clotilde Gaillard investigated the state of trivalent europium dissolved in RTILs as a function of anions in the RTILs and in the presence of added chloride anions.[19]

Here, we employed XAFS to study the component and structure of $ChCl-ZnCl_2$ ionic liquids at different $x(ZnCl_2)$, without destruction of the ionic liquid during the measurement. XAFS can be used to detect the local structure of the core atom. In our experiments, XAFS spectra of six kinds of $ChCl-ZnCl_2$ RTILs at different $x(ZnCl_2)$ were measured. The average coordination numbers and coordination distances of Zn species in the six kinds of $ChCl-ZnCl_2$ RTILs were calculated. The data shows that $x(ZnCl_2)$ has a regular influence on the coordination number and distance of Zn species. DSC was used to detect enthalpies of melting transition of different $ChCl-ZnCl_2$ RTILs, indicating the presence of three main Zn species, namely, $ZnCl_3^-$, $Zn_2Cl_5^-$, and Cl−Zn−Cl ion pair. Our results reveal that Cl−Zn−Cl ion pair is a main species at higher $x(ZnCl_2)$.

## 2. Experimental Section

**2.1. Materials.** The $ChCl-ZnCl_2$ RTILs were prepared according to the method reported by Abbott et al.[11] Six kinds of RTILs were prepared in molar fractions of $x(ZnCl_2) = 0.4$, 0.5, 0.6, 0.667, 0.714, and 0.75, respectively. Concentrated aqueous solution of $ZnCl_2$ was used as standard sample. All chemicals used were of analytical grade. After the volatile impurities (water, etc.) were removed by evaporation under vacuum at 30 °C overnight, the ionic liquids sealed in airtight glass tubes were incubated at −16 °C for 2 days to prepare the crystals.

**2.2. Methods.** The enthalpies of melting transition of different RTILs were measured by DSC (DSC-822e, Mettler-Toledo Corp.). The sample was scanned from −50 to 100 °C at a programmed rate of 5 °C/min. To achieve better effect for

* Corresponding authors. H.X.: 239 Zhang Heng Road, Pudong District, Shanghai, China, 201204; tel.: (86) 21-33933101(o); fax: (86) 21-33933031; e-mail: xuhongjie@sinap.ac.cn. G.W.: 2019 Jia Luo Road, Jiading District, Shanghai, China, 201800; tel. (86) 21-59554531(o); fax: (86) 21-59558905; e-mail: wuguozhong@sinap.ac.cn.

10.1021/jp809788u CCC: $40.75 
Published on Web 01/27/2009

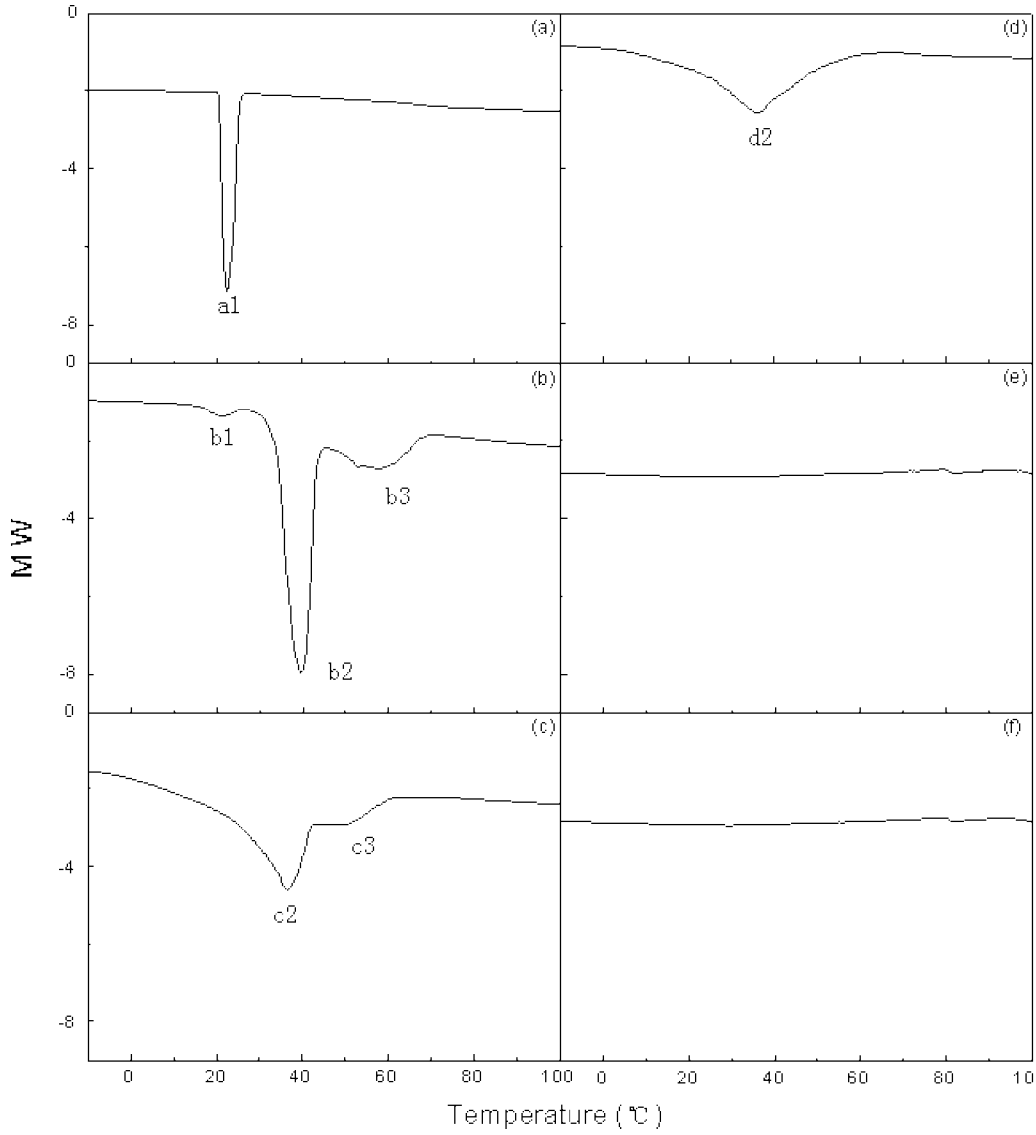


**Figure 1.** DSC heating curves for ChCl−$ZnCl_2$ ionic liquids at a scanrate of 5 °C/min. $x(ZnCl_2)$: (a) 0.4, (b) 0.5, (c) 0.6, (d) 0.667, (e) 0.714, (f) 0.75.

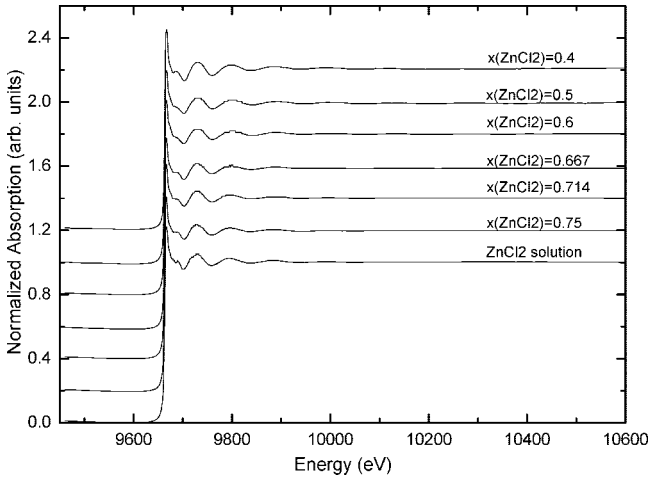


**Figure 2.** XAFS spectra of Zn species in ChCl−$ZnCl_2$ RTILs at different $x(ZnCl_2)$ and $ZnCl_2$ solution sample.

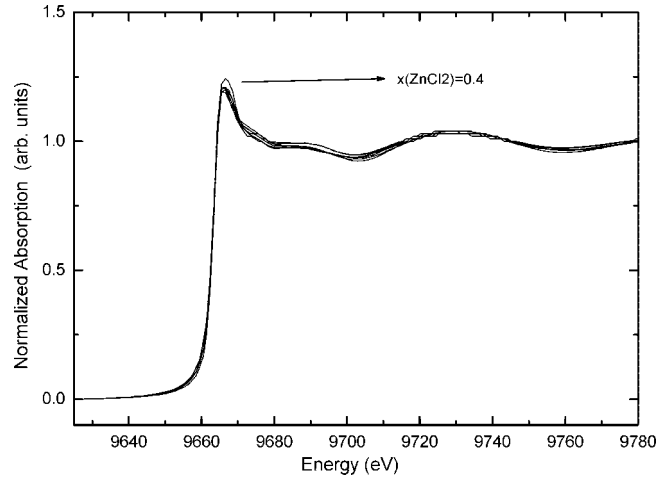


**Figure 3.** XANES spectra of Zn species in ChCl−$ZnCl_2$ RTILs at different $x(ZnCl_2)$.

crystallizing and measurement, the sample was held at −50 °C for 40 min. Liquid nitrogen cooling system in the DSC equipment was used to cool the sample from room temperature to −50 °C.

The XAFS measurement was carried out at the XAFS station of the BSRF (Beijing Synchrotron Radiation Facility) under normal storage ring conditions (2.2 GeV and 150−250 mA). Spectra were recorded at the Zn K-edge (9.659 keV) in

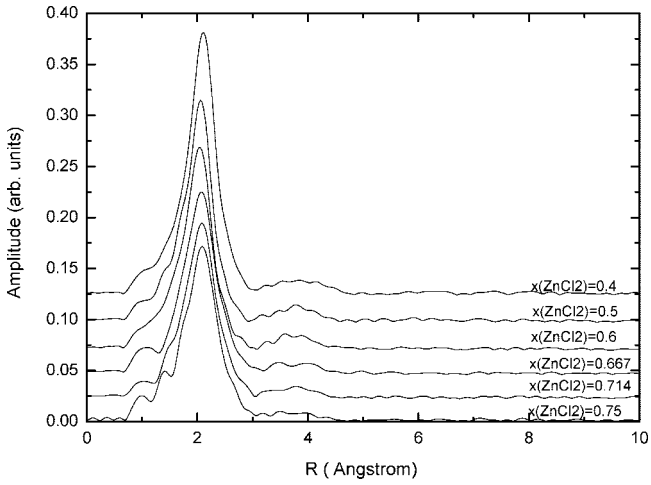


**Figure 4.** Fourier transforms of EXAFS data of Zn species in ChCl−$ZnCl_2$ RTILs at different $x(ZnCl_2)$.

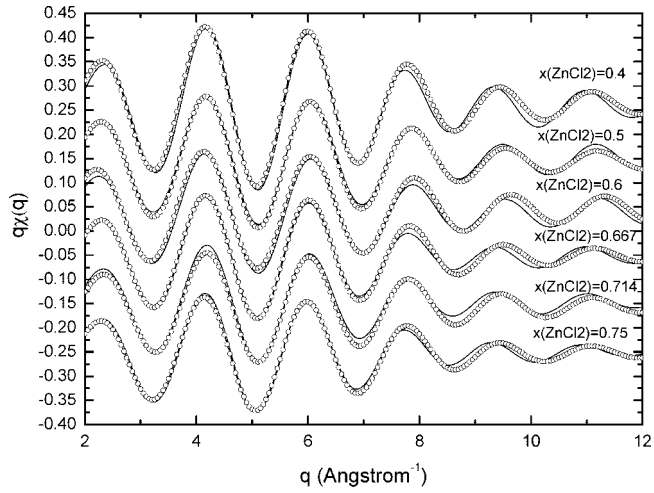


**Figure 5.** Fitting result in $q$ space of Zn species in ChCl−$ZnCl_2$ RTILs at different $x(ZnCl_2)$.

transmission mode using a Si(111) double-crystal monochromator. All of the samples were measured at room temperature. EXAFS (extended X-ray absorption fine structure) data was dealt by NSRL XAFS software packages. The threshold energy, $E_0$, was set to the maximum derivative point of the absorption edge. Background was removed by using the NSRLXAFS standard procedure.

For the highly disordered liquid systems like RTILs the Gaussian pairs distribution function is invalid to describe the nearest-neighbor atom distribution.[21−23] In the EXAFS fitting for obtaining the quantitative structural parameters, the pairs' distribution function $g(R)$ is commonly assumed as a convolution $P_G \otimes P_E$, where $P_G = (2\pi\sigma^2_t) - 1/2 \exp[-(R - R_j)^2/(2\sigma_t^2)]$ is used to describe the thermal disorder ($\sigma_t$) in a form of Gaussian function, and $P_E$ is used to describe the structural disorder ($\sigma_s$).

$$P_E(R) = \begin{cases} \frac{1}{2\sigma_s^3}(R - R_0)^2 \exp(-(R - R_0)/\sigma_s) & ;R \geq R_0 \\ 0 & ;R < R_0 \end{cases} \quad (1)$$

$R_0$ is the distance of the coordination atom which is mostly close to the center atom. The maximum distance is $R_0 + 2\sigma_s$, and the mean distance is $R_0 + \sigma_s$. The EXAFS function changes to the following formula:

$$\chi(k) = \sum_j \frac{N_j f_j(k) S_0^2(k)}{kR_{0j}^2} \exp(-2k^2\sigma_t^2) \times [1 + (2k\sigma_s)^2]^{-3/2} e^{-2R_{0j}/\lambda(k)} \times \sin[2kR_{0j} + \delta_j(k) + 2\varphi_C(k) + 3 \arctan(2k\sigma_s)] \quad (2)$$

The amplitude reduction factor is set to 0.79 by $ZnCl_2$ concentrated aqueous solution standard sample. The thermal disorder ($\sigma_t$) is fixed at the same value (0.04), which makes the fitting better than other parameters. The $k$ range of 2.5 to 12 $Å^{-1}$ was used in the Fourier transform. We used $k$-weight EXAFS $X(k)$ functions in the fitting for the chlorine atom. The phase and backscattering amplitude functions were generated with the FEFF 8.1 code.[24]

**TABLE 1: Local Structural Parameters of Zn Species in ChCl−$ZnCl_2$ RTILs at Different $x(ZnCl_2)$**

| $x(ZnCl_2)$ | $N$ | $\sigma_S$ | $R_0$ (Å) | $\sigma_t$ | $R$ factor |
|---|---|---|---|---|---|
| 0.4 | 3.0 | 0.06 | 2.17 | 0.04 | 0.05 |
| 0.5 | 2.9 | 0.09 | 2.14 | | 0.05 |
| 0.6 | 2.8 | 0.08 | 2.15 | | 0.05 |
| 0.667 | 2.6 | 0.09 | 2.15 | | 0.04 |
| 0.714 | 2.5 | 0.09 | 2.15 | | 0.04 |
| 0.75 | 2.4 | 0.09 | 2.16 | | 0.05 |

## 3. Results and Discussion

Figure 1 shows the DSC curves of six kinds of ChCl−$ZnCl_2$ RTILs. Figure 1a shows a melting peak at 22.5 °C at $x(ZnCl_2) = 0.4$, while Figure 1b shows three melting peaks at 21.2, 39.6, and 57.7 °C, respectively, at $x(ZnCl_2) = 0.5$. By increasing the $x(ZnCl_2)$ to 0.667, the DSC curve only shows one wide melting peak at 36.5 °C. At $x(ZnCl_2) = 0.714$ and 0.75, there is no melting peak. From the DSC curves in Figure 1, it can be affirmed that there are three kinds of peaks. The three peaks are at 21, 39, and 57 °C. The peak at 21 °C is only present in Figure 1, a and b, and the height of the peak decreases rapidly. The peak at 39 °C appears in Figure 1, b, c, and d, and the peak becomes weaker and wider with increasing of $x(ZnCl_2)$. The peak at 57 °C is much weaker than the peak at 39 °C at higher $x(ZnCl_2)$. Since the cooling process is different, the melting point and enthalpy of the ionic liquid are somewhat different from those found in the literature.[10,13]

Figure 2 shows XAFS spectra of Zn species in the six ChCl−$ZnCl_2$ RTILs as well as the concentrated $ZnCl_2$ aqueous solution. XAFS spectra of the seven samples seem similar, which indicate the coordination shells and atoms around Zn atom are similar. Figure 3 shows XANES spectra of Zn species in the six ChCl−$ZnCl_2$ RTILs. XANES spectra are sensitive to changes in the Zn inner coordination sphere. The intense edge resonance, positioned at 9664 eV, results from an electronic transition from a 1s core state to an empty 4p final state. The white line peak of the RTIL at $x(ZnCl_2) = 0.4$ is clearly higher than the white line peaks of other RTILs, indicating that the coordination environment of Zn species changes obviously when $x(ZnCl_2)$ changes from 0.4 to 0.5. The transition probabilities from 1s core states to empty 4p final states of Zn main species in the two RTILs are different. The DSC result also shows this change. There is only one distinct peak at 21 °C in Figure 1a. The same peak at 21 °C in Figure 1b nearly disappears, and another main peak at 39 °C appears. This indicates that the main

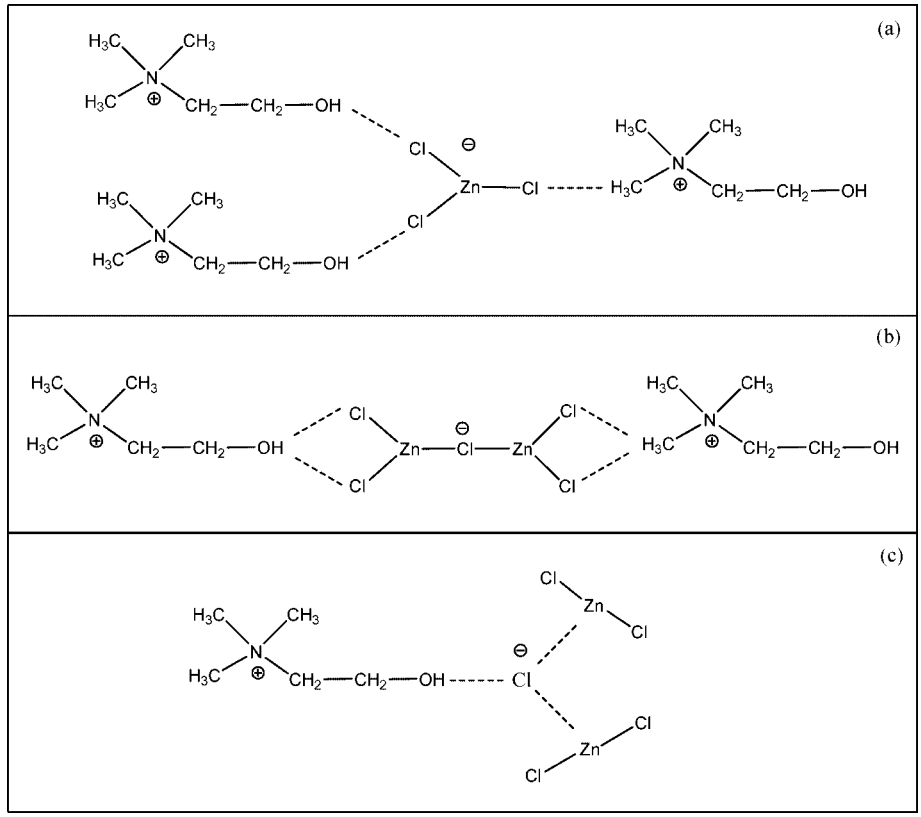


**Figure 6.** Structures of the three Zn species in $ChCl-ZnCl_2$ RTILs.

Zn species changes when $x(ZnCl_2)$ changes from 0.4 to 0.5, which accords with the change of XANES spectra. As $x(ZnCl_2)$ changes from 0.5 to 0.75, there is no remarkable change, implying that the five RTILs have similar coordination environments. Because the Zn species in RTILs are individual anions and RTILs system is a medium disorder system, XANES spectra of the six RTILs are almost structureless.

Figure 4 shows Fourier transforms of EXAFS data of Zn species in the six $ChCl-ZnCl_2$ RTILs. There are no structures at long distance, which also indicate that anions in the RTILs are individual. Fitting curves of inverse Fourier transform in $q$ space in Figure 5 indicate the fittings are acceptable. Table 1 shows the local structural parameters of the six different RTILs. In the RTILs at $x(ZnCl_2) = 0.4$, 0.5, 0.6, 0.667, 0.714, and 0.75, the coordination numbers of Zn species are 3.0, 2.9, 2.8, 2.6, 2.5, and 2.4, respectively. At $x(ZnCl_2) = 0.4$, the coordination number is 3.0, indicating that the coordination number of Zn species in this RTIL is 3.0. Compared to the DSC measurements and the literature,[10] the main Zn species in this RTIL is $ZnCl_3^-$. At $x(ZnCl_2) = 0.5$, the XANES spectrum and DSC curve are different from those at $x(ZnCl_2) = 0.4$, so we suggest that the main species at $x(ZnCl_2) = 0.5$ is $Zn_2Cl_5^-$ anion and the coordination number of Zn species in $Zn_2Cl_5^-$ anion is 3.0. As $x(ZnCl_2)$ increases, the coordination number continues to decrease. We presume that there is a new main species existing in the RTIL at higher $x(ZnCl_2)$. When $x(ZnCl_2)$ increases to 0.75, because the coordination number decreases to 2.4, we speculate that the new Zn species is the Cl−Zn−Cl ion pair whose coordination number is 2.0. This form of Zn species is in good agreement with the coordination number and the balance of ions and charges. Presence of the Cl−Zn−Cl ion pair also gives a good explanation to the DSC curves shown in Figure 1d−f.

From the DSC and XAFS analysis, $ZnCl_3^-$ is the exclusive dominant Zn species at $x(ZnCl_2) = 0.4$, and $Zn_2Cl_5^-$ is the maximum Zn species at $x(ZnCl_2) = 0.6$. When $x(ZnCl_2)$ is beyond 0.667, Cl−Zn−Cl ion pairs become the dominant Zn species. Using the enthalpies of melting transition and coordination numbers, the compositions of different crystals and Zn species at different $x(ZnCl_2)$ are calculated as illustrated in Table 2. From the above analysis, Cl−Zn−Cl ion pair plays an important role in the structure of the RTILs. In Figure 6 we speculate that there are three kinds of local structures in $ChCl-ZnCl_2$ RTILs at different $x(ZnCl_2)$. In $ZnCl_3^-$ anion, the three Cl atoms form an equilateral triangle, and the Zn atom is located in the center of the equilateral triangle. $Ch^+$ cations and $ZnCl_3^-$ anions interact with each other through hydrogen bonds, due to the interionic Coulomb forces, as shown in Figure 6a. These interactions, although relatively weak, seem to direct the orientation between ions and might govern the overall assembly. In $Zn_2Cl_5^-$ anion, a bridge Cl atom connects the two Zn atoms, and the other four Cl atoms are allotted to the two Zn atoms averagely, as shown in Figure 6b.The main interactions between $Ch^+$ cations and $Zn_2Cl_5^-$ anions are also through hydrogen bonds. Because the bridge bond between Zn atom and Cl atom

**TABLE 2: Composition of Different Zn Species in $ChCl-ZnCl_2$ RTILs at Different $x(ZnCl_2)$**

| | | | | percentage of | | |
|---|---|---|---|---|---|---|
| $x(ZnCl_2)$ | coordn no. | $T_m$ (°C) | $\Delta H_m$ (J $g^{-1}$) | different crystals | $ZnCl_3^-$ and $Zn_2Cl_5^-$ | Cl−Zn−Cl ion pairs |
| 0.4 | 3.0 | 22.5 | 22.33 | 1.00 (1) | 1 | − |
| 0.5 | 2.9 | 21.2 | 2.17 | 0.08 (1) | 0.9 | 0.1 |
| | | 39.6 | 83.87 | 0.66 (2) | | |
| | | 57.7 | 21.10 | 0.16 (3) | | |
| 0.6 | 2.8 | 36.5 | 60.50 | 0.32 (2, 3) | 0.8 | 0.2 |
| | | 50.4 | | | | |
| 0.667 | 2.6 | 36.5 | 44.40 | 0.18 (2, 3) | 0.6 | 0.4 |
| 0.714 | 2.5 | − | − | − | 0.5 | 0.5 |
| 0.75 | 2.4 | − | − | − | 0.4 | 0.6 |

is rotatable, the system seems to be more disordered. When Cl−Zn−Cl ion pair exists in ChCl−$ZnCl_2$ RTILs, it interacts with $ZnCl_3^-$, $Zn_2Cl_5^-$, and dissociative $Cl^-$ anions through Coulomb forces, and the dissociative $Cl^-$ anion can appear in several Cl−Zn−Cl ion pairs and $Ch^+$ cations, as shown in Figure 6c.

In our experiments, the calculated coordination parameters and enthalpies of melting transition of different Zn species in ChCl−$ZnCl_2$ RTILs are dependent on $x(ZnCl_2)$. The result is indicative of the complex interactions between choline chloride and chlorozincate anions. The chemical formula of Zn species in RTIL at $x(ZnCl_2) = 0.4$ can be $[Ch]^+ZnCl_3^-$. When $x(ZnCl_2)$ changes to 0.5 and 0.6, both $[Ch]^+ZnCl_3^-$ and $[Ch]^+Zn_2Cl_5^-$ are observed. When $x(ZnCl_2)$ is 0.667, another main new Zn species, Cl−Zn−Cl ion pairs, largely appear in the RTIL. When $x(ZnCl_2)$ is beyond 0.714, Cl−Zn−Cl ion pairs are predominant in the ionic liquid.

## 4. Conclusions

A detailed XAFS and DSC analysis has been performed to investigate the species and local structures of Zn species in ChCl−$ZnCl_2$ RTILs. By analyzing coordination environment and enthalpies of melting transition, we characterized the forms and structural parameters of three main Zn species, $ZnCl_3^-$, $Zn_2Cl_5^-$, and Cl−Zn−Cl ion pair at different $x(ZnCl_2)$.

**Acknowledgment.** This work was supported by the National Natural Science Foundation of China (grant no. 10705046 and 20673137) and CAS Innovation Program. We are grateful to the persons of XAFS beamlines in Beijing Synchrotron Radiation Facility and Hefei National Synchrotron Radiation Laboratory in China for the XAFS beam time.

## References and Notes

(1) Welton, T. *Chem. Rev.* **1999**, *99*, 2071. Dupont, J.; de Souza, R. F.; Suarez, P. A. Z. *Chem. Rev.* **2002**, *102*, 3667.

(2) Baudequin, C.; Baudoux, J.; Levillain, J.; Cahard, D.; Gaumont, A.-C.; Plaquevent, J.-C. *Tetrahedron: Asymmetry* **2003**, *14*, 3081.

(3) Wasserscheid, P.; Keim, W. *Angew. Chem., Int. Ed.* **2000**, *39*, 3772.

(4) Welton, T. *Chem. Rev.* **1999**, *99*, 2071.

(5) Earle, M. J.; Seddon, K. R. *Pure Appl. Chem.* **2000**, *72*, 1391.

(6) Ranke, J.; Stolte, S.; Störmann, R.; et al. *Chem. Rev.* **2007**, *107*, 2183–2206.

(7) Rivera, A.; Rössler, E. A. *Phys. Rev. B* **2006**, *73*, 212201.

(8) Lapkin, A. A.; Plucinski, P. K.; Cutler, M. *J. Nat. Prod.* **2006**, *69*, 1653–1664.

(9) Ranke, J.; Stolte, S.; Störmann, R.; et al. *Chem. Rev.* **2007**, *107*, 2183–2206.

(10) Tokuda, H.; Ishii, K.; Bin Hasan Susan, M. A.; et al. *J. Phys. Chem. B* **2006**, *110*, 2833–2839.

(11) Abbott, A. P.; Capper, G.; Davies, D. L.; et al. *Inorg. Chem.* **2004**, *43*, 3447.

(12) Abbott, A. P.; Capper, G.; McKenzie, K. J.; et al. *J. Electroanal. Chem.* **2007**, *599*, 288–294.

(13) Abbott, A. P.; Griffith, J.; Nandhra, S. *Surf. Coatings Technol.* **2007**.

(14) Yaodong, L.; Guozhong, W.; Mingying, Q. *J. Crystal Growth* **2005**, *281*, 616–622.

(15) Hsiu, S.-I.; Huang, J.-F.; I-Wen, S.; et al. *Electrochim. Acta* **2002**, *47*, 4367–4372.

(16) Abbott, A. P.; Capper, G.; Davies, D. L.; et al. *Inorg. Chem.* **2005**, *44*, 6497–6499.

(17) Abbott, A. P.; Capper, G.; Davies, D. L.; et al. *J. Chem. Eng. Data* **2006**, *51*, 1280–1282.

(18) Jensen, M. P.; Dzielawa, J. A.; Rickert, P.; et al. *J. Am. Chem. Soc.* **2002**, *124*, 10664–10665.

(19) Gaillard, C.; Billard, I.; Chaumont, A.; et al. *Inorg. Chem.* **2005**, *44*, 8355.

(20) Visser, A. E.; Jensen, M. P.; Laszak, I.; et al. *Inorg. Chem.* **2003**, *42*, 2197.

(21) Zheng, W.; Zhongrui, Li.; Zhen, J.; et al. *J. Alloys Compd.* **2007**, .

(22) Newville, M.; Livin, P.; Yacoby, š. Y.; Rehr, J. J.; Stern, E. A. *Phys. Rev. B* **1993**, *47*, 14126.

(23) Zhong, W. J.; Wei, S. Q. *J. Univ. Sci. Technol. China* **2001**, *31*, 328.

(24) Burchardt, T.; Hansen, V.; Valand, T. *Electrochim. Acta* **2001**, *46*, 2761.

JP809788U